Lab on a Chip

Lysis and Direct Detection of Coliforms on Printed Paper-based Microfluidic Devices

Journal:	*Lab on a Chip*
Manuscript ID	LC-ART-06-2020-000665.R1
Article Type:	Paper
Date Submitted by the Author:	08-Sep-2020

Complete List of Authors:	Snyder, Sarah; University of Michigan, Ann Arbor, Materials Science and Engineering Boban, Mathew; University of Michigan, Materials Science and Engineering Li, Chao; University of Wisconsin Madison, Biomedical Engineering VanEpps, J. Scott; University of Michigan, Ann Arbor, Biointerfaces Institute, Emergency Medicine Mehta, Geeta; University of Michigan, Ann Arbor, Materials Science and Biomedical Engineering Tuteja, Anish; University of Michigan, Materials Science and Engineering

Lysis and Direct Detection of Coliforms on Printed Paper-based Microfluidic Devices

Sarah A. Snyder[1,2], *Mathew Boban*[2,3], *Chao Li*[1,2], *J. Scott VanEpps*[2,4*], *Geeta Mehta*[1,3,5*], *Anish Tuteja*[1,2,3,6*].

[1]Department of Materials Science and Engineering,
[2]Biointerfaces Institute,
[3]Department of Macromolecular Science and Engineering
[4]Department of Emergency Medicine,
[5]Department of Biomedical Engineering,
[6]Department of Chemical Engineering,

University of Michigan, Ann Arbor, MI 48109

*Corresponding authors: Email: jvane@umich.edu; mehtagee@umich.edu; atuteja@umich.edu

Keywords: paper-based microfluidics, cell lysis, *E. coli* detection

Abstract:

Coliforms are one of the most common families of bacteria responsible for water contamination. Certain coliform strains can be extremely toxic, and even fatal if consumed. Current technologies for coliform detection are expensive, require multiple complicated steps, and can take up to 24 hours to produce accurate results. Recently, open-channel, paper-based microfluidic devices have become popular for rapid, inexpensive, and accurate bioassays. In this work, we have created an integrated microfluidic coliform lysis and detection device by fabricating customizable omniphilic regions via direct printing of omniphilic channels on an omniphobic, fluorinated paper. This paper-based device is the first of its kind to demonstrate successful cell lysing on-chip, as it can allow for the flow and control of both high and low surface tension liquids, including different cell lysing agents. The fabricated microfluidic device was able to successfully detect *E. coli*, via the presence of the coliform-specific enzyme, β-galactosidase, at a concentration as low as $\sim 10^4$ CFU/mL. Further, *E. coli* at an initial concentration of 1 CFU mL^{-1} could be detected after only 6 hours of incubation. We

believe that these devices can be readily utilized for real world *E. coli* contamination detection in multiple applications, including food and water safety.

Introduction:

The coliform, *Escherichia coli,* is a major pathogen worldwide due to its ability to cause fatal diarrheal and extraintestinal diseases.[1] Currently, the 'gold standards' for the determination of *E. coli* contamination are methods that use automated polymerase chain reaction (PCR) and fluorescence detection.[2] While these systems can provide accurate results within 24 hours, they rely on expensive, complex instrumentation, as well as user expertise. With the numerous recent food safety incidents involving *E. coli* and *Listeria monocytogenes*, there has been a significant interest in developing novel detection devices to not only reduce the cost of *E. coli* detection on a food-handling surface, but to also decrease the contamination detection time. Within the last ten years, paper-based microfluidic devices have gained significant popularity due to their inexpensive nature and wide range of potential applications. Such devices can also be flexible, simple to dispose, easy to scale up, facile to fabricate, and biocompatible.[3] Current paper-based devices for *E. coli* detection utilize a variety of mechanisms for rapid detection, including gold nanoparticle aggregation,[4, 5] Mie scattering,[6] and microfluidic origami.[7] However, these techniques can involve several complicated fabrication and experimental steps, including nanoparticle functionalization, antibody conjugation, and several paper folding and unfolding steps. One of the major reasons for these complicated steps is the inability of the fabricated devices to conduct cell lysis on chip. This inability stems from the difficulty in containing and directing low surface tension cell lysing agents within the fabricated microfluidic channels. Although lysis on a chip has been demonstrated for closed-channel microfluidic devices, using methods such as, thermal, chemical, droplet digital, mechanical, electroporation and laser[8-10], none of these techniques have been published for open-channel paper-based devices. We recently demonstrated a simple, cheap device fabrication methodology to contain low surface tension liquids on paper.[11] However, while the

channels could contain low surface tension liquids, they were unable to facilitate significant flow rates with high surface tension liquids (such as water or cell culture medium), due to the relatively low surface energy of the fabricated channels. These high flow rates are essential for the cell lysis reagent mixing, and coliform detection over a short time period. In this report, we discuss a new methodology for making omniphilic channels that incorporate photoactive titanium dioxide. This new device architecture allows us to fabricate microfluidic devices that can not only contain and direct low surface tension media, but also maintain very high flow rates with high surface tension liquids. With these capabilities combined, we fabricated the first ever, all-in-one coliform lysis and colorimetric detection device that can be employed as an affordable, portable detector for water or food contamination.

Our paper-based microfluidic devices are fabricated by directly printing omniphilic (wettable by all liquids, *i.e.* contact angle < 90°)[12] channels on an omniphobic[13-17] (non-wettable by all liquids, *i.e.* contact angle > 90°) background. On most surfaces, a range of contact angles can be measured, from a maximum advancing contact angle when liquid is added to a droplet on the surface, to a minimum receding contact angle when liquid is removed from the droplet.[13, 16] Maximizing the advancing contact angle of the non-wettable background maximizes its capacity to confine a low surface tension liquid within the wettable channel. Similarly, minimizing the receding contact angle in the wettable domains allows for the retention and high flow rates of the contacting liquid.

To engineer our paper-based devices, we leveraged two key surface properties: surface energy and texture. We produced a low surface energy, rough background by covalently bonding a fluorinated silane to a fibrous paper substrate, rendering it omniphobic. The choice of paper used for fabricating the devices was crucial, as the paper texture must facilitate omniphilic channel printing, while maintaining the high advancing contact angles necessary for liquid confinement. After comparing various paper substrates, including different cellulose-based filter papers, we selected a cheap, commercially available copy / printing

paper (see methods) for fabricating our microfluidic devices. The paper, designed for ensuring good printing on inkjet and laserjet printers, was composed of large, flat fibers (**Figure 1d**). This texture ensured a relatively high liquid-solid contact area, and allowed for the easy and direct printing of our omniphilic channels. To fabricate the omniphilic channels, we selectively printed an omniphilic ink onto the omniphobic paper substrate. To minimize defects, the ink solution needed to leave a complete film when printed across the substrate, that is, it needed to exhibit a low receding contact angle on top of the low surface energy omniphobic paper substrate. Further, the ink needed to adhere to the underlying omniphobic paper in a short period of time, and maintain its adherence to the substrate even when soaked with both high and low surface tension liquids. To achieve this functionality, we developed a high surface energy, nanotextured ink composed of titanium dioxide (TiO_2) nanoparticles dispersed within an adhesive polyurethane (see methods). TiO_2 is a well-known photocatalyst that undergoes a hydrophilic conversion upon UV irradiation.[18] After UV exposure, the TiO_2 printed channels facilitated high flow rates flow with both low and high surface tension liquids (**Figure 1b**). **Figure 1a** summarizes all the fabrication steps, while Figure 1c shows the printing equipment used for fabricating our paper-based microfluidic devices. The deposited omniphilic channels (**Figure 1d**) allowed a variety of liquids with high and low surface tensions to be contained within the omniphilic domains (**Figure 1e,f**). Further, the controlled deposition of the TiO_2 based ink allowed for the fabrication of microfluidic channels of any desired configuration (**Figure 1g**).

To detect *E. coli* contamination, we utilized chlorophenol red-β-D-galactopyranoside (CPRG) as the reaction substrate for the enzyme, β-galactosidase (β-gal). β-gal is an enzyme present inside all coliforms, including *E. coli.* When β-gal cleaves the glycosidic bond within the CPRG substrate, the CPRG is converted to chlorophenol red, with an accompanying color change from vibrant yellow to a deep red.[19] Previous work has utilized a similar approach on different paper-based devices to detect *E. coli* at a concentration of 10^1 colony forming units

(CFU) mL^{-1} in 4 hours, or at a concentration of 10^7 CFU mL^{-1} within 30 minutes.[9, 20, 21] However, these devices require at least two separate steps for *E. coli* detection: lysing the bacterial cells to release the β-gal enzyme off-chip, and subsequently adding the lysed cells to the paper-based device for detection. This is due to the fact that, as discussed previously, most paper-based microfluidics systems cannot contain low surface tension lysis reagents for extended periods.[22] Further, as discussed above, although recently developed paper-based devices have shown the capability to contain low surface tension liquids, they are typically unable to ensure high flow rates for both low and high surface tension liquids.[11, 20, 23-28]

The first step in our device / channel design is to ensure mixing between the lysing and the cell containing solutions. Due to the low Reynolds number laminar flow within microfluidic channels ($R_e \approx 2.25$; assuming fluid density $\rho = 1{,}000$ kg m^{-3}, fluid velocity $u = 1$ mm s^{-1}, the channel width $L = 2$ mm, and kinematic viscosity of water $\mu = 8.9 \times 10^{-11}$ Pa s), it is difficult to achieve complete, homogenous mixing of the two liquids. Therefore, we designed our device with two inlets leading into a serpentine mixing zone that ends at a detection patch. We simulated how adding 2, 3, 4 or 7 turns to the serpentine mixing zone affects the mixing of the two fluid streams with a simplified COMSOL model of the central section of the device. **Figure 2a** shows the concentration profiles obtained for the 0 and 7 turn open-channel devices. It is clear that increasing the number of turns in the serpentine mixing section effectively increases the mixing between the two fluid streams.

Next, we fabricated five devices with different number of turns to experimentally validate the mixing effectiveness of the serpentine regions. We added water, dyed yellow and blue, into the two device inlets. The results, shown in **Figure 2b**, exhibit that, as expected, adding more turns in the serpentine region increased mixing between the two liquid streams. There was a clearly defined interface in the detection region of the 0 turn device, and as more turns were added, that interface became less defined, until the two streams were almost

entirely mixed in the detection region of the 7 turn device. This matched the trends observed in the COMSOL model.

We also tested the mixing capability of all five devices for the *E. coli* assay by adding Luria-Bertani (LB) broth (the bacterial growth medium), in one inlet and blue-dyed Bacterial Protein Extraction Reagent (B-PER II – the lysis buffer), in the other, as shown in **Figure 2c**. These results followed the same trend as those in **Figure 2b**, however, the two streams appeared to effectively mix within fewer turns when compared to the number of turns it took for the two dyed water streams to mix. This can be attributed to the Marangoni flow, which can significantly increase mass transport across an interface with a surface tension gradient.[29] In this case, the Marangoni flow occurs due to the significant surface tension difference between the LB Broth ($\gamma_{lv} \approx 72$ mN m^{-1}) and the B-PER II extraction reagent ($\gamma_{lv} \approx 31$ mN m^{-1}).

To optimize the design of the lysis-on-a-chip assay, we also evaluated two different detection patch shapes: circles and diamonds. The shape of the detection patch can be a significant contributor to the overall detection limit of the fabricated device. This is because as the bacterial medium and the cell lysing solution evaporate from the detection patch, the solids dissolved within these liquids get concentrated at the edges of the detection patch, due to the so called coffee-ring effect.[30] Thus the ratio between the perimeter of the edges and the surface area of the detection patch (essentially the surface area / volume ratio, but ignoring the thickness of the detection patch) becomes a significant design parameter for the fabricated device.

Figure 3a shows a schematic of all Red, Green, and Blue (RGB) colors. The colors within the white box represent all possible colors that can be observed in our assay, as it transforms from a bright yellow to a deep red. The initial yellow color comes from the CPRG reagent, and when β-gal cleaves the glycosidic bond within CPRG, there is an accompanying color change to a deep red. **Figure 3b** shows the bright field images of the circular and

diamond shaped patches, along with their respective processed images via thresholding. A white pixel indicates a pixel with RGB values within the limits specified in **Figure 3a** (R >140, G < 200, and B < 200). It is immediately clear that the diamond shaped patch has more white pixels or 'hits' when compared to the circular detection patch. **Figure 3c** plots the number of white pixels per unit area for both the circle and the diamond shaped patches. The statistically significant (p = 0.0228) difference in counts can be attributed to the increased perimeter to surface area ratio of the diamonds. For circles, the perimeter to surface area ratio is $2\pi r/\pi r^2 = 2/r$, where r is the radius of the detection patch. On the other had for diamonds, the ratio is $4l/l^2 = 4/l$, where l is the edge length for the diamond.

To perform the lysis-on-a-chip assay, *E. coli* in LB broth with isopropyl β-D-1-thiogalactopyranoside (IPTG, a lactose-like molecule used to induce β-gal production)[31] and B-PER II were added to their respective inlets in the 7 turn mixing devices, as shown in **Figure 3d.** The 7 turn serpentine channel devices allowed for a residence time of about one minute, providing both diffusion across the interface and chaotic advection as mechanisms for mixing.[32] **Figure 3d** shows the time-lapse images of the *E. coli* (at a concentration of ~10^7 CFU mL^{-1}) mixing with the lysis buffer in the serpentine region of the device and the resultant color change after the solution reaches the detection patch. A color change initially becomes observable within 5 minutes after the liquid reaches the detection patch, and the change nearly reaches completion after about 15 minutes in the patch. Thus, the devices were not only able to contain the lysis buffer, but they successfully lysed the *E. coli*, releasing the β-gal within the cells and causing the CPRG to become chlorophenol red.

For real-world applications, coliform detection devices need to be sensitive to much lower bacterial concentrations.[33] To address this issue, we incubated 1 CFU mL^{-1} of *E. coli* in LB at 37°C and tested the resulting culture at various time points. **Figure 3e** shows the growth curve with the corresponding color changes and processed images at different time points. After 6 hours of incubation, with ~10^4 CFU/mL bacteria present in solution, the color change

become apparent to the naked eye, and obvious in the processed images. Therefore, with minimal incubation time (~ 6 hours), our fabricated paper-based devices were able to detect bacterial concentrations of 1 CFU mL^{-1}, a concentration that has immense applicability for field detection of bacterial contamination. Additionally, without any incubation, the devices were capable of detection bacterial concentrations as low as ~10^4 CFU/mL.

In summary, in this work, we have fabricated an all-in-one paper-based device that can lyse and detect pathogenic *E. coli* within minutes. The device was composed of omniphilic channels fabricated on omniphobic paper with a direct printing technique, allowing for the rapid mask-less fabrication of arbitrary channel geometries. The fabricated device was able to detect a dilute sample at only 1 CFU mL^{-1} by incubation for 6 hours prior to introduction to the device. Without any incubation, the devices were capable of detection bacterial concentrations as low as ~10^4 CFU/mL. While the device fabricated here was tailored for *E. coli* detection, the ability to lyse cells on chip is expected to provide a completely new functionality to open-channel paper-based microfluidic devices, opening the door for a wide range of potential biomedical applications. Given that the paper-based device developed in this work does not feature any external pumping mechanism in the process of lysis or detection, this device can be easily deployed in the field.

Experimental Section

Substrate preparation: To produce a substrate resistant to wetting by most liquids, copy paper was reacted with a low surface energy fluorinated silane. The paper (Boise X-9 Multiuse OX9001, OfficeMax) pore size is ~ 50 microns, and the paper thickness was ~ 0.1mm. The paper was pre-treated with oxygen plasma to enhance reactivity (Harrick Plasma PDC-001, 250 mTorr, 30 W, 30 min). It was then placed into a vacuum oven held at <5 mmHg, 70 °C for 24 h with 400 μL of fluorosilane (heptadecafluoro-1,1,2,2-tetrahydrodecyl trichlorosilane, Gelest). The fluorosilane reacts with the hydroxyl groups on the plasma treated cellulose,

rendering it non-wettable by most liquids. The advancing/receding contact angles were 153/0° and 113/0° for water and hexadecane, respectively.

Ink preparation: The omniphilic ink was composed of 70 wt.% TiO_2 and 30 wt.% polyurethane adhesive, dissolved at a concentration of 25 mg mL^{-1} in acetone (Fisher Scientific), and agitated with a probe ultrasonicator (Heat Systems XL-2020) until evenly dispersed. Anatase titanium dioxide nanopowder (32 nm) was obtained from Alfa Aesar. Aleene's Fabric Fusion permanent fabric adhesive, a water-borne polyurethane, was used as the binder.

Device fabrication: Pieces of the fluorinated paper were adhered to glass slides with solvent resistant double-sided tape (3M 9629PC) and placed onto a leveled heated stage (~70 °C) in a lab-built printing apparatus (**Figure 1b**). This consisted of an XYZ motion stage (Shapeoko 2) holding a tapered polypropylene dispensing nozzle (20 gauge or 610 μm outer diameter, McMaster-Carr) connected via polytetrafluoroethylene tubing (1/32" inner diameter, McMaster-Carr) to a syringe pump (KD Scientific Model 200) dispensing the solution at 2.25 mL h^{-1} from a glass syringe. The motion and operation of the pump and XYZ stage were computer-controlled with GCODE commands, which were generated from design files produced in Inkscape, an open-source vector drawing software. This apparatus allows the mask-free patterning of arbitrary polymer solutions on a variety of substrates with ~500 μm resolution. Two passes were performed to ensure uniform coverage of the TiO_2 ink on the fluorinated paper. Once deposited, the ink was exposed to 254 nm UV light in a sterilizer cabinet (purchased from Salon Sundry) for 5 hours to render it wettable by all liquids prior to use.

Device testing: Dynamic contact angles were measured on the fluorinated paper with a Ramé-Hart 200-F1 goniometer, using the sessile drop technique. Dyed deionized water, hexadecane (Alfa Aesar), 3 wt.% aqueous solutions of Triton X-100 (MP Biomedicals) and sodium dodecyl sulfate (Hoefer) surfactants, and 2X B-PER Bacterial Protein Extraction Reagent

(Fisher Scientific) were used to test the capacity of the printed devices to contain a broad range of liquids (**Figure 1d, 1e**). The pendant drop method was used to measure the surface tensions of these liquids with the goniometer.

Design of cell lysis device: An approximate model of the cell lysis device was generated in COMSOL 5.2 to guide the design of the channel to ensure thorough mixing of the cell lysis reagents and the *E. coli*, in order to enhance the reproducibility and speed of the assay. The central segment of the device was modeled as a laminar flow channel, with a no-slip boundary condition at the solid-liquid contact at the channel base, and a slip boundary condition for the liquid-air interfaces at the top and sides. A chemical species was introduced at one inlet of the flow channel, and its concentration was plotted to evaluate the effectiveness of mixing of various geometries. The results were compared to photographs taken of aqueous food-dye solutions (McCormick) mixing in the channels.

Bacterial culture and growth: Colonies of *E. coli* (UTI89) were grown overnight at 37°C onto LB broth (Lennox) agar (from Fisher Scientific) plates and all colonies were used within two weeks of growth. To perform experiments, one colony scraped from the LB agar plate was grown in LB Broth on a shaker at 37°C with 10 mM isopropyl β-D-1-thiogalactopyranoside (IPTG, purchased from Invitrogen). When the optical density at 600 nm reached 0.6 ± 0.1 (measured with an Ultrospec 2100 pro UV/Visible Spectrophotometer), indicating an approximate concentration of 10^7 colony forming units (CFU) mL^{-1}, the *E. coli* were tested on the serpentine devices. Here, the term colony forming units is used in place of number of cells because although a cell may be viable, it is not necessarily culturable. The total concentrations of cells in all experiments performed were quantified by simultaneously plating on an LB agar plate for colony enumeration while testing the devices.

For the sensitivity tests, one colony was grown in LB until the optical density reached 0.6 ± 0.1. This culture was serially diluted down to approximately 10^2 CFU mL^{-1} and 1 mL was placed into 99 mL of sterile LB, yielding an effective cell concentration of 1 CFU mL^{-1}.

The *E. coli* were incubated with 10 mM IPTG and samples were taken out at various time points. At each time point, the withdrawn sample was used to measure optical density and to induce a color change on the diamond shaped devices.

Lysis-on-a-chip assay: 1 μL of chlorophenol red-*β*-D-galactopyranoside (CPRG) (purchased from Sigma-Aldrich) dissolved in 2X Bacterial Protein Extraction Reagent (B-PER, purchased from Fisher Scientific) at a concentration of 3 mg mL^{-1} was placed in the detection region of the device and allowed to evaporate. *E. coli* in LB and 2X B-PER were pipetted into their respective inlets and were allowed to wet the omniphilic regions of the device. Characterization images were taken on a Nikon D3200 camera with fixed exposure and lighting settings.

Image thresholding: All thresholding was performed in MATLAB R2014a. Counted, white pixels indicate RGB values where $R > 140$, $G < 200$, and $B < 200$ while black pixels indicated RGB values outside of those limits. Statistical analysis was performed with a standard two-sample t-test.

Acknowledgements

This work was supported by the DOD OCRP Early Career Investigator Award W81XWH-13-1-0134 (GM) and DOD Pilot award W81XWH-16-1-0426 (GM). Research reported in this publication was supported by the National Cancer Institute of the National Institutes of Health under award number P30CA046592 and the National Institute of Allergy and Infectious Diseases of the National of the National Institutes of Health under award number AI128006.

Author Contributions: All authors edited and approved the final version of the manuscript. Conceptualization, JSV, GM, and AT; Data curation, SAS, MB; Formal analysis, SAS, MB; Software, MB; Funding acquisition, GM, AT, JSV; Investigation, SAS, MB; Methodology, SAS, MB, CL; Project administration, GM, AT, JSV; Resources, GM, AT, JSV; Supervision,

GM, AT, JSV; Validation, SAS, MB; Visualization, SAS, GM, AT, JSV; Writing – original draft, SAS, MB, CL, GM, AT; Writing – review & editing, GM, AT, JSV.

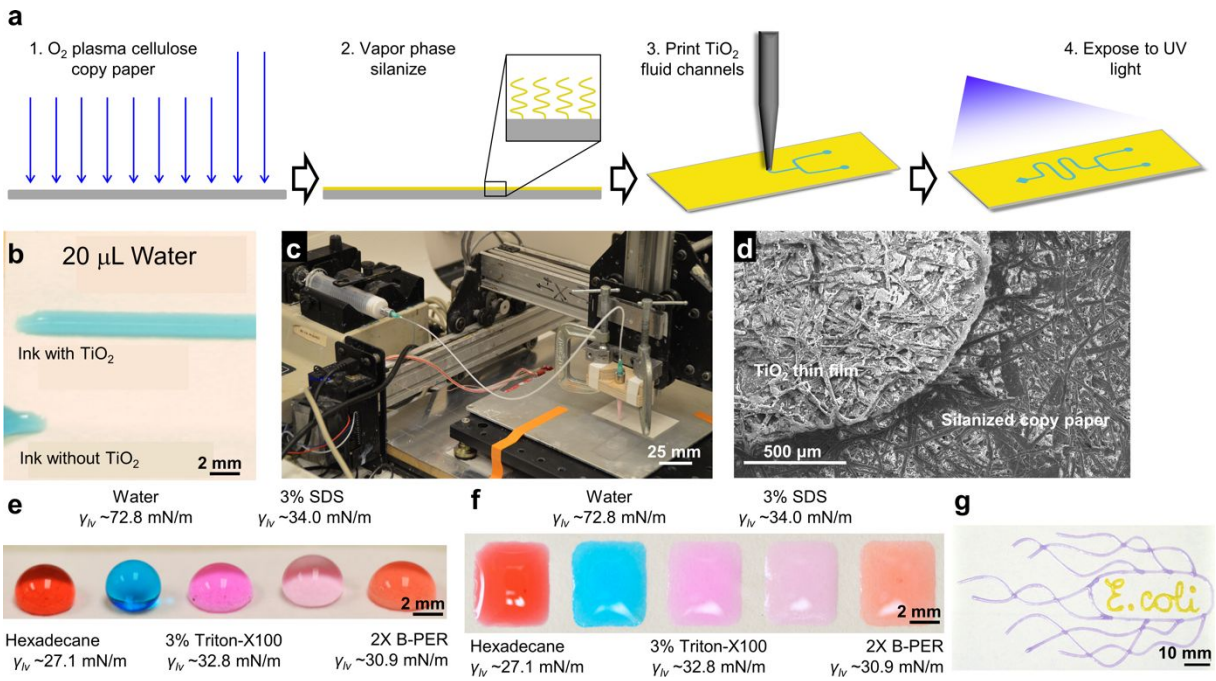

Figure 1. The fabrication and characterization of the paper-based *E. coli* detection devices. **a)** The steps required to manufacture a complete *E. coli* detection device, including O_2 plasma cleaning, vapor phase silanization with a fluorinated silane, printing of the TiO_2 channels and exposure of the devices to 254 nm UV light. **b)** 20 µL of dyed-water wetting channels printed with and without ink containing TiO_2. The UV activated TiO_2 containing ink allows high surface energy water to easily wet the channel. **c)** The omniphilic channel printing apparatus developed using an XYZ stage can be utilized to print any device design. **d)** An SEM image shows the TiO_2 thin film on top of the silanized copy paper. **e & f)** Liquid drops repelled and contained on the omniphobic and superomniphilic regions, respectively. **g)** A channel in the shape of a single *E. coli* bacterium filled with dyed silicone oil (γ_{lv} = 22 mN/m), demonstrates the ability to confine low surface tension liquids and to print any desired microfluidic channel shape with this technique.

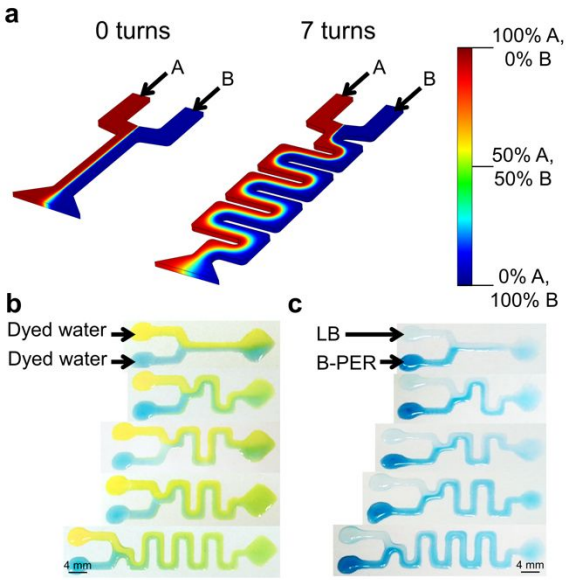

Figure 2. Optimization of device design to achieve complete mixing. **a)** Concentration profiles generated from COMSOL models of lysis devices with zero or seven turns in the mixing channel. Dark red represents a 100% concentration of liquid A and dark blue represents a 100% concentration of liquid B. **(b-c)** Images demonstrating the effective mixing in the serpentine region of the device with **(b)** dyed water and **(c)** LB and 2X B-PER. The addition of more turns in the serpentine region increased mixing, allowing for nearly homogenous mixing in the 7-turn device.

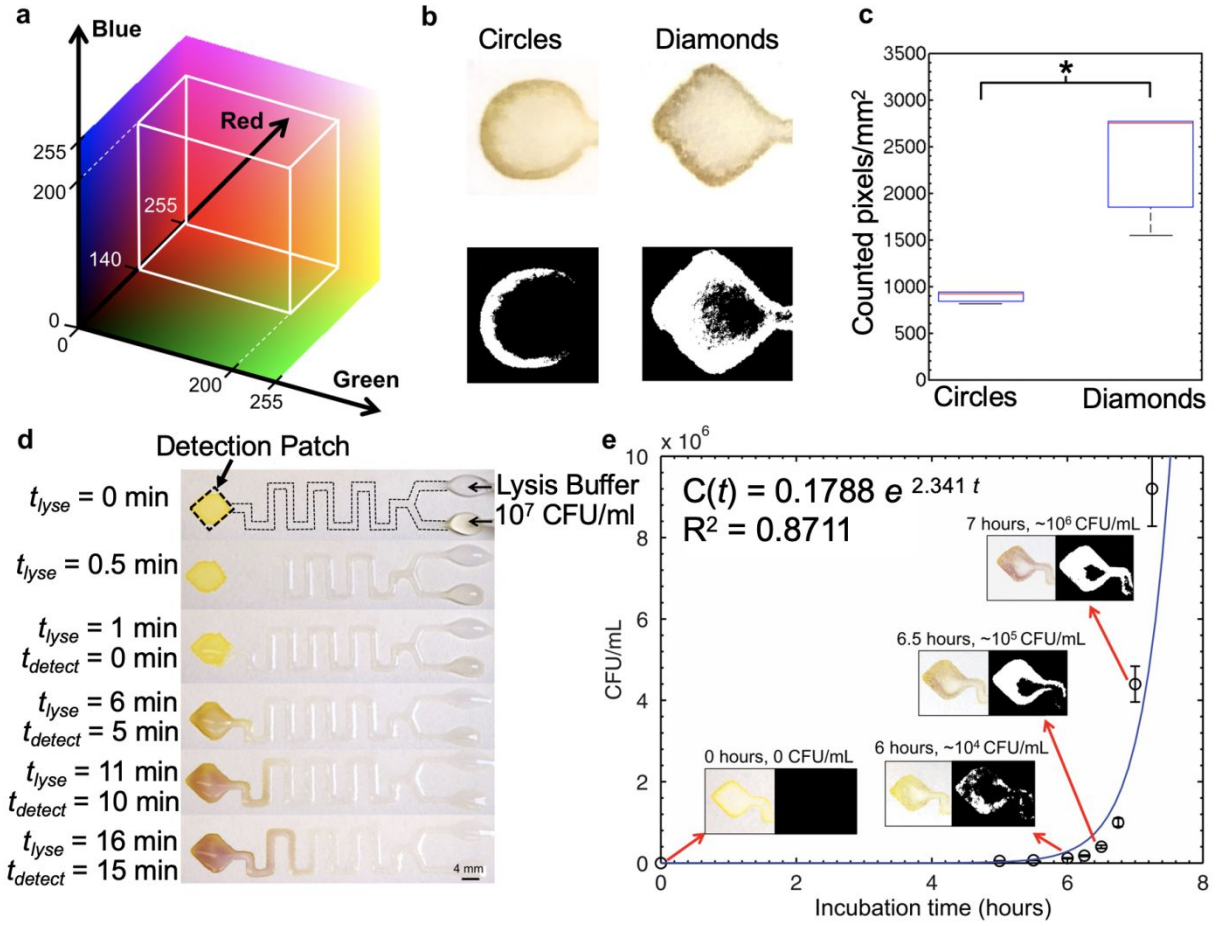

Figure 3. *E. coli* lysis and detection results on different paper-based devices. **a)** RGB schematic with a white outlined box showing the colors contained within the thresholding limits of R >140, G < 200, and B < 200. All pixels with RGB values within those limits indicate a color change and are counted, and pixels with RGB values outside those limits are ignored. **b)** Bright field images and corresponding processed images via thresholding for both circular and diamond shaped detection patches. **c)** Counted pixels per unit area of the processed images for both circular and diamond shaped detection patches. With a higher number of counted pixels, diamond shaped detection patches exhibit a statistically significant (p = 0.0228) increase in sensitivity compared to circular detection patches. **d)** *E. coli* lysed on chip at a concentration of ~10^7 CFU mL^{-1} with the *E. coli* inlet, 2X B-PER lysis buffer inlet and the CPRG detection patch labeled. The *E. coli* spent approximately 1minute mixing with the lysis buffer in the serpentine region before reaching the detection patch, and there was a noticeable color change within 5 minutes at the detection patch. After 15 minutes, the color

change nearly reached completion. **e)** The growth curve and corresponding color change images with their respective processed images on the lysis devices for ~1 CFU mL^{-1} incubated in medium over time. With a minimal detection limit of ~10^4 CFU/mL after 6 hours of incubation, there was a noticeable onset of color change.

References:

1. Croxen, M.; Law, R.; Scholz, R.; Keeney, K.; Wlodarska, M.; Finlay, B., Clinical Microbiology Reviews. *Clin. Microbiol. Rev.* **2013,** *26* (4), 822-880.

2. Baeumner, S. N. A., Trends and opportunities in food pathogen detection. *Anal Bioanal Chem* **2008,** *391*, 451-454.

3. Rolland, J. P.; Mourey, D. A., Paper as a novel material platform for devices. *MRS bulletin* **2013,** *38* (4), 299-305.

4. Shafiee, H.; Asghar, W.; Inci, F.; Yuksekkaya, M.; Jahangir, M.; Zhang, M. H.; Durmus, N. G.; Gurkan, U. A.; Kuritzkes, D. R.; Demirci, U., Paper and flexible substrates as materials for biosensing platforms to detect multiple biotargets. *Scientific reports* **2015,** *5*, 8719.

5. Li, C.-z.; Vandenberg, K.; Prabhulkar, S.; Zhu, X.; Schneper, L.; Methee, K.; Rosser, C. J.; Almeide, E., Paper based point-of-care testing disc for multiplex whole cell bacteria analysis. *Biosensors and Bioelectronics* **2011,** *26* (11), 4342-4348.

6. San Park, T.; Yoon, J.-Y., Smartphone detection of Escherichia coli from field water samples on paper microfluidics. *IEEE Sensors Journal* **2014,** *15* (3), 1902-1907.

7. Govindarajan, A.; Ramachandran, S.; Vigil, G.; Yager, P.; Böhringer, K., A low cost point-of-care viscous sample preparation device for molecular diagnosis in the developing world; an example of microfluidic origami. *Lab on a Chip* **2012,** *12* (1), 174-181.

8. Nan, L.; Jiang, Z.; Wei, X., Emerging microfluidic devices for cell lysis: a review. *Lab on a Chip* **2014,** *14* (6), 1060-1073.

9. Adkins, J. A.; Boehle, K.; Friend, C.; Chamberlain, B.; Bisha, B.; Henry, C. S., Colorimetric and Electrochemical Bacteria Detection Using Printed Paper- and Transparency-Based Analytic Devices. *Anal Chem* **2017,** *89* (6), 3613-3621.

10. Kang, D.-K.; Ali, M. M.; Zhang, K.; Huang, S. S.; Peterson, E.; Digman, M. A.; Gratton, E.; Zhao, W., Rapid detection of single bacteria in unprocessed blood using Integrated Comprehensive Droplet Digital Detection. *Nature Communications* **2014,** *5* (1), 5427.

11. Li, C.; Boban, M.; Snyder, S. A.; Kobaku, S. P.; Kwon, G.; Mehta, G.; Tuteja, A., Paper‐Based Surfaces with Extreme Wettabilities for Novel, Open‐Channel Microfluidic Devices. *Advanced Functional Materials* **2016,** *26* (33), 6121-6131.

12. Kobaku, S. P.; Kota, A. K.; Lee, D. H.; Mabry, J. M.; Tuteja, A., Patterned Superomniphobic‐Superomniphilic Surfaces: Templates for Site‐Selective Self‐Assembly. *Angewandte Chemie International Edition* **2012,** *51* (40), 10109-10113.

13. Kota, A. K.; Choi, W.; Tuteja, A., Superomniphobic surfaces: Design and durability. *MRS Bulletin* **2013,** *38* (05), 383-390.

14. Pan, S.; Kota, A. K.; Mabry, J. M.; Tuteja, A., Superomniphobic Surfaces for Effective Chemical Shielding. *Journal of the American Chemical Society* **2012**.

15. Tuteja, A.; Choi, W.; Ma, M. L.; Mabry, J. M.; Mazzella, S. A.; Rutledge, G. C.; McKinley, G. H.; Cohen, R. E., Designing superoleophobic surfaces. *Science* **2007,** *318*, 1618-1622.

16. Tuteja, A.; Choi, W.; Mabry, J. M.; McKinley, G. H.; Cohen, R. E., Robust omniphobic surfaces. *Proceedings of the National Academy of Sciences* **2008,** *105* (47), 18200-18205.

17. Wooh, S.; Vollmer, D., Silicone brushes: omniphobic surfaces with low sliding angles. *Angewandte Chemie International Edition* **2016,** *55* (24), 6822-6824.

18. Hashimoto, K.; Irie, H.; Fujishima, A., TiO2 photocatalysis: a historical overview and future prospects. *Japanese journal of applied physics* **2005,** *44* (12R), 8269.

19. Tallon, P.; Magajna, B.; Lofranco, C.; Leung, K. T., Microbial indicators of faecal contamination in water: a current perspective. *Water, air, and soil pollution* **2005,** *166* (1-4), 139-166.

20. Jokerst, J. C.; Adkins, J. A.; Bisha, B.; Mentele, M. M.; Goodridge, L. D.; Henry, C. S., Development of a paper-based analytical device for colorimetric detection of select foodborne pathogens. *Analytical chemistry* **2012,** *84* (6), 2900-2907.

21. Wang, J.; Monton, M. R. N.; Zhang, X.; Filipe, C. D.; Pelton, R.; Brennan, J. D., Hydrophobic sol–gel channel patterning strategies for paper-based microfluidics. *Lab on a Chip* **2014,** *14* (4), 691-695.

22. Lisowski, P.; Zarzycki, P. K., Microfluidic paper-based analytical devices (μPADs) and micro total analysis systems (μTAS): development, applications and future trends. *Chromatographia* **2013,** *76* (19-20), 1201-1214.

23. Glavan, A. C.; Martinez, R. V.; Subramaniam, A. B.; Yoon, H. J.; Nunes, R. M.; Lange, H.; Thuo, M. M.; Whitesides, G. M., Omniphobic "RF paper" produced by silanization of paper with fluoroalkyltrichlorosilanes. *Advanced Functional Materials* **2014,** *24* (1), 60-70.

24. Lan, W.-J.; Maxwell, E. J.; Parolo, C.; Bwambok, D. K.; Subramaniam, A. B.; Whitesides, G. M., based electroanalytical devices with an integrated, stable reference electrode. *Lab on a Chip* **2013,** *13* (20), 4103-4108.

25. Rajendra, V.; Sicard, C.; Brennan, J. D.; Brook, M. A., Printing silicone-based hydrophobic barriers on paper for microfluidic assays using low-cost ink jet printers. *Analyst* **2014,** *139* (24), 6361-6365.

26. Schutzius, T. M.; Elsharkawy, M.; Tiwari, M. K.; Megaridis, C. M., Surface tension confined (STC) tracks for capillary-driven transport of low surface tension liquids. *Lab on a Chip* **2012,** *12* (24), 5237-5242.

27. Yamada, K.; Henares, T. G.; Suzuki, K.; Citterio, D., Paper‐based inkjet‐printed microfluidic analytical devices. *Angewandte Chemie International Edition* **2015,** *54* (18), 5294-5310.

28. Zhang, Y.; Ren, T.; Li, T.; He, J.; Fang, D., Paper‐Based Hydrophobic/Lipophobic Surface for Sensing Applications Involving Aggressive Liquids. *Advanced Materials Interfaces* **2016,** *3* (22), 1600672.

29. Scriven, L.; Sternling, C., The marangoni effects. *Nature* **1960,** *187* (4733), 186-188.

30. Deegan, R. D.; Bakajin, O.; Dupont, T. F.; Huber, G.; Nagel, S. R.; Witten, T. A., Capillary flow as the cause of ring stains from dried liquid drops. *Nature* **1997,** *389* (6653), 827-829.

31. Jobe, A.; Bourgeois, S., Lac represser-operator interaction: VIII. Lactose is an anti-inducer of the lac operon. *Journal of molecular biology* **1973,** *75* (2), 303-313.

32. Glavan, A. C.; Martinez, R. V.; Maxwell, E. J.; Subramaniam, A. B.; Nunes, R. M.; Soh, S.; Whitesides, G. M., Rapid fabrication of pressure-driven open-channel microfluidic devices in omniphobic RF paper. *Lab on a Chip* **2013,** *13* (15), 2922-2930.

33. Rompré, A.; Servais, P.; Baudart, J.; De-Roubin, M.-R.; Laurent, P., Detection and enumeration of coliforms in drinking water: current methods and emerging approaches. *Journal of microbiological methods* **2002,** *49* (1), 31-54.

Table of Contents Image